Dynamic Light Scattering
<paper review>

Osamu Katagiri-Tanaka
A01212611@itesm.mx

7 May, 2020

Three different methods were used to determine the size and size distribution of PBCA nanoparticles (nanoparticles formed by anionic emulsion polymerization of butylcyanoacrylate in the presence of poloxamer 188 as a stabilizer).

	scanning electron microscopy SEM	dynamic light scattering DLS	analytical ultracentrifugation AUC
Particle diameter	167 nm	199 nm	184 nm
advantages	detailed shape and morphological information	short time and low cost	measurements can be obtained at low particle concentrations
		the movement of particles in a centrifuge (ANUC) shows a stronger size dependence than the diffusion coefficient (DLS)	
disadvantages	risk of changes in particle properties during drying and contrasting	measurement will be identical or ~larger than the 'real' particle	sedimentation of nanoparticles shall be slow enough to obtain sufficient data points

A. Bootz, V. Vogel, D. Schubert, J. Kreuter, Comparison of scanning electron microscopy, dynamic light scattering and analytical ultracentrifugation for the sizing of poly(butyl cyanoacrylate) nanoparticles, Eur. J. Pharm. Biopharm. 57 (2004) 369–375. https://doi.org/10.1016/S0939-6411(03)00193-0.

Research paper

Comparison of scanning electron microscopy, dynamic light scattering and analytical ultracentrifugation for the sizing of poly(butyl cyanoacrylate) nanoparticles

Alexander Bootz[a], Vitali Vogel[b], Dieter Schubert[b], Jörg Kreuter[a],*

[a]Institut für Pharmazeutische Technologie, Johann Wolfgang Goethe-Universität, Frankfurt, Germany
[b]Institut für Biophysik, Johann Wolfgang Goethe-Universität, Frankfurt, Germany

Abstract

Nanoparticles represent promising carriers for controlled drug delivery. This work focuses on the size and molecular mass characterization of polyalkylcyanoacrylate nanoparticles formed by anionic emulsion polymerization of butylcyanoacrylate in the presence of poloxamer 188 as a stabilizer. Three different methods were used to determine the size and size distribution of the particle populations: scanning electron microscopy (SEM), dynamic light scattering (DLS), and analytical ultracentrifugation (ANUC). SEM on freeze-dried and Au-shadowed samples showed a relatively narrow distribution of virtually spherical particles with a mean diameter of 167 nm. DLS yielded a monomodal distribution with hydrodynamic diameters around 199 nm (in the absence of additional stabilizer) or 184 nm (in the presence of 1% poloxamer 188). The size distribution determined by ANUC using sedimentation velocity analysis was somewhat more complex, the size of the most abundant particles being around 184 nm. Molar particle mass distributions centered around 2.3×10^9 g/mol. The advantages and disadvantages of the three sizing techniques are discussed.
© 2003 Elsevier B.V. All rights reserved.

Keywords: Nanoparticles; Polyalkylcyanoacrylate; Particle size; Molecular weight; Analytical ultracentrifugation; Dynamic light scattering; Electron microscopy

1. Introduction

The objective in developing drug delivery systems is to achieve high drug concentrations in diseased tissue and low concentrations in healthy tissue and the rest of the body. Nanoparticles offer a possibility to achieve this goal. Enhancement of therapeutic efficacy and reduction of toxic side effects have been demonstrated for a variety of drugs bound to such particles [1,2].

Over the past few years many studies have focussed on the use of poly(butyl cyanoacrylate) (PBCA) nanoparticles as carriers for a number of different drugs (e.g. doxorubicin, cyclosporin A, MRZ 2/596, a novel NMDA-receptor-antagonist) [3–6]. Their physicochemical characterization has been the objective of a large number of investigations [7–10]. However, the structure of the nanoparticles formed by the agglomeration of the polymer chains is not yet fully described.

For intravenous administration of nanoparticles a mean particle diameter < 200 nm and a narrow size distribution is desirable to avoid the risk of embolism and to enable sterile filtration (0.22 μm). A knowledge of particle size, therefore, is an essential requirement. The present study compares three different methods to determine the mean size and the size distribution of particles formed by PBCA: scanning electron microscopy (SEM), dynamic light scattering (DLS) [also called photon correlation spectroscopy (PCS)] and analytical ultracentrifugation (ANUC).

While SEM allows an analysis of the morphological appearance of the particles, DLS and ANUC enable a description of the size distribution of the particles and an estimation of the molar particle mass, in particular with spherical particles. This paper also discusses the advantages and disadvantages of the three techniques.

* Corresponding author. Institut für Pharmazeutische Technologie, Johann Wolfgang Goethe-Universität, Marie-Curie-Strasse 9, 60439 Frankfurt, Germany. Tel.: +49-69-798-29682; fax: +49-69-798-29694.
E-mail address: kreuter@em.uni-frankfurt.de (J. Kreuter).

2. Materials and methods

2.1. Materials

n-Butyl-2-cyanoacrylate (Sicomet® 6000) was obtained from Sichel-Werke (Hannover, Germany), poloxamer 188 (Pluronic F-68) was from Sigma (Steinheim, Germany). All other chemicals were purchased from Merck (Darmstadt, Germany).

2.2. Preparation of nanoparticles

Particles were prepared by anionic emulsion polymerization [11] of 1% (w/v) butylcyanoacrylate in 0.01 N HCl under constant stirring with a magnetic stirrer at 500 rpm; 1% (w/v) poloxamer 188 was used as a stabilizer. Polymerization was assumed to be complete after 4 h [10]. After that time the nanoparticle suspension was neutralized with 0.1 N NaOH. The suspension was filtered through a sintered glass filter with a pore size of 90–150 μm (Schott, Mainz, Germany). The final nanoparticle content was assessed by gravimetry: Free poloxamer 188 was removed by pelleting the particles by centrifugation at $16,000 \times g$ for 40 min and discarding the supernatant. The pellet was resuspended in distilled water. An aliquot (100 μl) of the dispersion was dried at 100 °C for 2 h and the residual was weighed using a supermicro balance (Sartorius, Göttingen, Germany).

The particles were stored at 4 °C and used without further purification. The size of the nanoparticles in suspension was stable for up to 8 months [12]. The same batch was used for the parallel experiments with the three techniques. The reproducibility of the preparation was determined by comparing the diameter and polydispersity (PD) of six independent batches by DLS.

2.3. Determination of density and viscosity of the solvents

Solvent density ρ was measured in a PAAR DMA 48 densitometer (Anton Paar GmbH, Graz, Austria). Solvent viscosity η was determined with a Cannon-Fenske capillary viscosimeter (VWR International GmbH, Darmstadt, Germany). The measurements were carried out at 20 °C. The results obtained with the two 0.9% (w/w) NaCl solutions used, containing either 0.05 or 1.0% (w/v) poloxamer 188, were ρ = 1.0044 and 1.0047 g/ml, and η = 1.00 and 1.27 mPa/s, respectively.

2.4. Scanning electron microscopy (SEM)

The nanoparticle suspension was diluted with distilled water (1:4) and applied to a metallic sample plate. The sample was freeze-dried, metallized with gold and investigated with a field emission EM, Hitachi S-45000 SEM, at 15 kV and a working distance of 15 mm. The diameter of the nanoparticles was measured using the software Paint Shop Pro 5 (Jasc Software, Eden Prarie, USA).

2.5. Particle size measurement by dynamic light scattering (DLS)

The particle size was measured using a Malvern Zetasizer $3000HS_A$ (Malvern, Worcs., UK) equipped with a 10-mW He–Ne laser (633 nm) and operating at an angle of 90° and a temperature of 20 °C. The samples of PBCA nanoparticles were diluted 1:20 with a 0.9% (w/w) solution of NaCl in distilled water to eliminate the primary charge effect. A sample volume of 2 ml was used in 10-mm-diameter cuvettes (Sarstedt, Germany). To determine the influence of the poloxamer 188 concentration on the measured particle size, in some experiments poloxamer 188 was added to the diluted samples to obtain a final concentration of 1% (w/v).

The mean hydrodynamic diameter of the particles, d_h, was computed from the intensity of the scattered light using the Malvern software package by multiple mode analysis, based on the theory of Brownian motion and the Stokes–Einstein equation:

$$D = \frac{kT}{3\pi\eta d_h} \qquad (1)$$

where D is the diffusion coefficient (the primary parameter obtained from DLS measurements), k the Boltzmann constant, T the temperature, and η the solvent viscosity. Good fits to the data were obtained assuming monomodal size distributions.

2.6. Particle size measurement by analytical ultracentrifugation (ANUC)

Analogous to sample preparation for measurements of dynamic light scattering, the sample was diluted 1:20 with a 0.9% (w/w) NaCl solution in distilled water, with or without addition of 1% (w/v) poloxamer 188. Optical turbidity was between 0.3 and 0.5 at 420 nm in a cuvette with an optical path length of 1 cm.

The sedimentation velocity experiments were carried out as described earlier [13], using a Beckman Optima XL-A ultracentrifuge (Munich, Germany), an An-50Ti rotor, and double-sector charcoal-filled Epon centerpieces of 12-mm optical path length. The rotor speed was 3000 or 4000 rpm and the rotor temperature 20 °C. Apparent absorbance (turbidity) versus radius data $A(r,t)$ were collected at 420 nm, using a radial step size of 0.01 nm. The data were modeled as a distribution of non-diffusing particles using the $l - sg^*(s)$ variant of the program sedfit [14,15]. If advantageous, the sedimentation coefficients s_{20} were transformed to standard conditions and given as $s_{20,w}$ [16].

2.7. Partial specific volume of nanoparticles

The partial specific volume (reciprocal density) of the nanoparticles, $\bar{v}$, is an important parameter in their characterization and is also required for the calculation of

the particle mass. $\bar{v}$ was determined from sedimentation velocity experiments of the nanoparticles in H_2O/D_2O mixtures with different densities, by plotting the sedimentation coefficient s_m in the maximum of the sedimentation coefficient distribution as a function of the density ρ of the medium and extrapolating the dependence $s_m(\rho)$ to $s_m = 0$ ('buoyant density method', [17,18]). $\bar{v}$ is the reciprocal of the corresponding solvent density.

2.8. Calculation of the diameter and the molar mass of the particles

For solid spherical particles, $g^*(s)$ curves obtained by the $l - sg^*(s)$ method can be converted into (relative) concentration-versus-diameter curves applying Eqs. (2)–(4):

$$s = \frac{M(1 - \bar{v}\rho)}{N_a f} \tag{2}$$

$$M = \frac{1}{6}\pi d^3 \frac{1}{\bar{v}} \tag{3}$$

$$f = 3\pi\eta d \tag{4}$$

where M is the molar particle mass, N_a, Avogadro's number, f, frictional coefficient of the particles, and d the particle diameter. Apparent diameters will be larger for less compact particles.

Particle masses can be obtained by an additional transformation applying Eq. (3). For the maximum of the $g^*(s)$ distribution, the corresponding molar mass can be determined without the 'solid sphere' assumption, by combining s_{20} and the average diffusion coefficient D_{20}, as obtained from DLS, via the Svedberg Eq. (5):

$$s = \frac{MD(1 - \bar{v}\rho)}{RT} \tag{5}$$

This calculation is, however, based on the assumption that the D-value used is a fair approximation for the Svedberg constant of the particles in the peak of $g^*(s)$.

3. Results

3.1. Morphology and size distribution of the particles by SEM

The nanoparticle suspensions were investigated by SEM without further purification. A typical micrograph is shown in Fig. 1. As shown in the figure, the most prominent property of the particles is their almost perfect spherical shape. The size distribution, determined from 156 particles, is given in Fig. 2. As compared to those of other nanoparticles intended for drug delivery (see, e.g. [13,19]) it is relatively narrow, > 90% of the particle diameters being in the range 145–190 nm. The mean diameter (number average) is 167 nm and virtually identical to the value for the maximum of the distribution. The standard deviation of
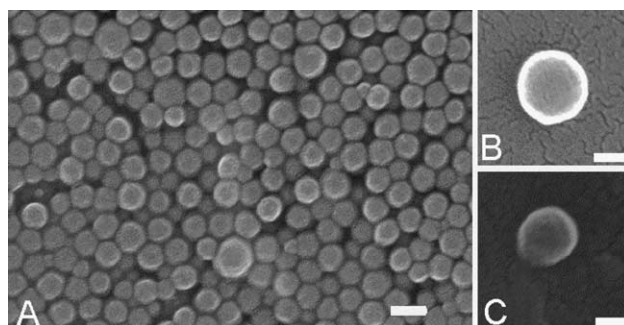

Fig. 1. Morphology of the PBCA nanoparticles (originally in H_2O), determined by SEM. (A) Densely packed particles; (B) and (C) isolated particles at higher magnification. Bar: 200 nm (A), 100 nm (B) and (C).

the mean is ± 16 nm. It should be noted that the measured particle diameters may be affected by shrinking during sample preparation.

3.2. Particle size distribution from DLS

DLS measurements require a larger number of particles (several orders of magnitude greater) compared to SEM, and thus provide much better statistics. They primarily yield diffusion coefficient distributions which, however, can be transformed into distributions of hydrodynamic diameters d_h [20]. For spherical particles, as under study here, d_h will be identical or somewhat higher than the values determined from SEM. However, with heterogeneous populations the weighting procedure will be different, so that differences between the results of the two methods will be inevitable.

Using the same particle batch as in Section 3.1, DLS measurements performed both without or with supplementary addition of poloxamer 188 yielded the size distributions shown in Fig. 3. Without further addition of stabilizer [i.e. at a poloxamer 188 concentration of 0.05% (w/v)], a mean intensity weighted diameter of 199 nm was found (PD 0.022). At a stabilizer concentration of 1% (w/v)
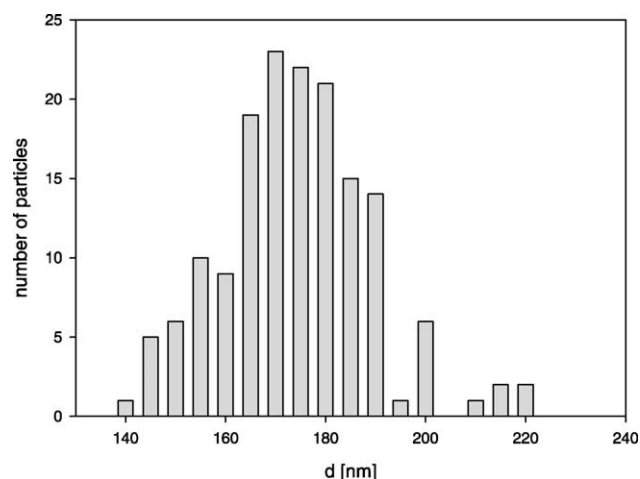

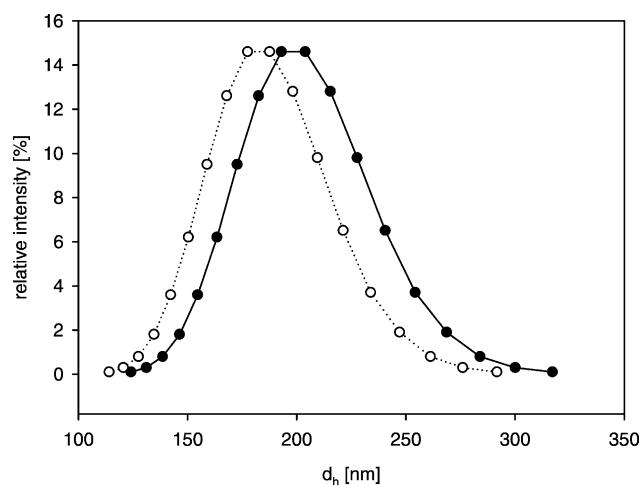Fig. 2. Distribution of particle diameters derived from Fig. 1a.

Fig. 3. Distribution of the (hydrodynamic) diameter d_h of the PBCA nanoparticles, in 0.05% (●) or 1 % (○) poloxamer 188, as measured by DLS.

the mean diameter was 184 nm (PD 0.034). The difference between the two values may be due to the presence of small amounts of aggregates in the former sample. In view of the difficulties involved, the agreement with the SEM results is good or at least satisfactory.

To ensure the reproducibility of the preparation method the average particle diameter, measured by DLS, and the yield of six independent PBCA nanoparticle batches was also compared. The mean particle diameter was (215 ± 17) nm and the yield (49 ± 6)%. Thus, reproducibility and yield of the preparation process appears to be good.

3.3. Determination of the size distribution of the particles by sedimentation velocity analysis

In contrast to protein nanoparticles intended for drug delivery that were studied recently [13,19,21], the sedimentation of the produced PBCA nanoparticles in water is slow enough to obtain sufficient data points for the sedimentation velocity analysis. Typical sedimentation velocity data on the latter particles, together with the curves fitted by the $l - sg^*(s)$ method [14], are shown in Fig. 4.
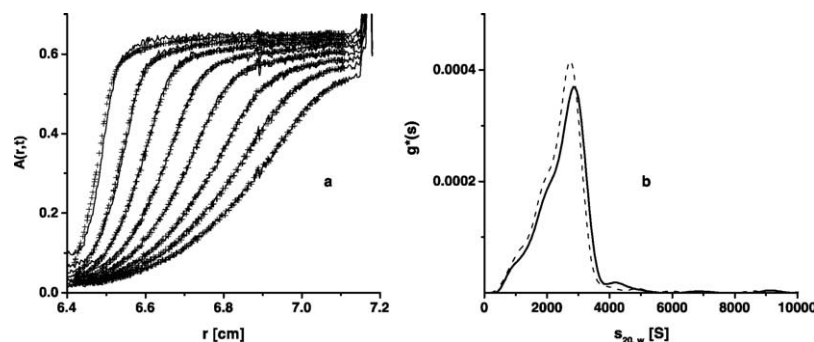
According to Fig. 4a, the fits are of reasonable quality, thus confirming the 'ideal and non-diffusing' model [14]. The distributions of the normalized values for the sedimentation coefficient, $g^*(s_{20,w})$, for samples in 0.05% and 1% (w/v) surfactant, are given in Fig. 4b. The two curves are virtually identical to each other. Their shape clearly indicates that the particle size distribution is somewhat more complex than suggested by the DLS measurements: besides a mean peak sedimenting with $s_{20,w}$-values around 2800 S there are at least two more slowly sedimenting components (with $s_{20,w}$-values around 1000 and 2000 S); there is also some more rapidly sedimenting material. Nevertheless the distributions are much less heterogeneous then found recently, by the same method, with other types of nanoparticles intended for drug delivery [13,19,21].

The conversions described below, from $s_{20,w}$-distributions to distributions of diameter and molar mass, require knowledge of the partial specific volume of the particles, $\bar{v}$. This was determined by the 'buoyant density method' with D_2O as a 'densifier' [18,22,23], plotting s_{20} of the peak of $g^*(s)$ versus solvent density ρ instead of M_{eff} from sedimentation equilibrium runs [17,18] (Fig. 5). It is obvious from the figure that particle density is virtually unaffected by the presence of 1% detergent, which suggests that little detergent binding to the particle takes place. The resulting $\bar{v}$-value is 0.871 ml/g in both cases.

Taking into account (i) the finding from SEM that the particles are spherical and (ii) the $\bar{v}$-value of the particles determined above the $g^*(s)$-curves of Fig. 4b can be converted into (relative) concentration-versus-diameter curves. The transformation is shown in Fig. 6 for both curves in Fig. 4b. The amplitudes of the curves do not represent true relative particle concentrations but are distorted by differences in light scattering for smaller and larger particles, respectively. However, as shown recently this effect is small for particles with narrow size distributions [13]. The d-values corresponding to the maxima of the curves, 185 and 183 nm, respectively, can thus safely be compared to the values derived from SEM, 167 nm and from DLS, 184 and 199 nm. It is apparent that the agreement is satisfactory.
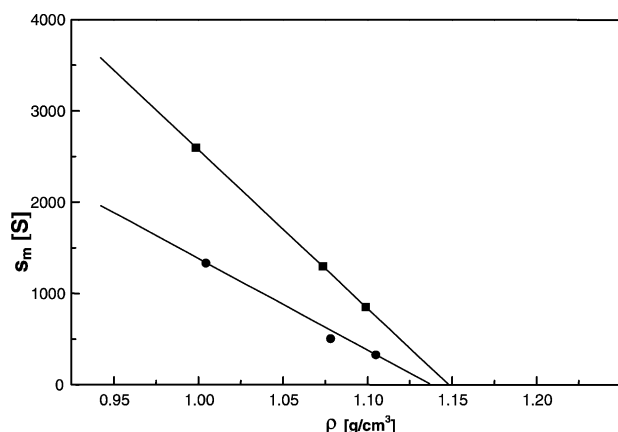

Fig. 4. Sedimentation velocity analysis of PBCA nanoparticles: (a) Experimental absorbance-versus-radius data, $A(r,t)$, for a sample containing 0.05% (w/v) poloxamer 188 (+), and curve fitted to them by direct boundary modeling (—). (b) Sedimentation coefficient distribution $g^*(s_{20,w})$ of the sample of Fig. 4a (——) and of another one containing 1% poloxamer 188 (–––). Particle concentration: approx. 0.25 mg/ml. Rotor speed: 4000 rpm.

Fig. 5. Determination of v̄, for PBCA nanoparticle samples containing 0.05% (□) or 1% (○) poloxamer 188, in H_2O/D_2O mixtures (plus 150 mM NaCl): sedimentation coefficient s_m at the maximum of the $g^*(s)$ distribution versus solvent density ρ. Particle concentration: approx. 0.25 mg/ml.

3.4. Estimation of the molar mass of the particles

In principle, the $c(d)$-curves of Fig. 6 can be transformed into concentration-versus-mass curves; however, the weighting procedure involved will render that part of the curve corresponding to the larger masses rather unreliable. We have therefore restricted ourselves to determining the molar particle mass corresponding to the maximum of $g^*(s)$. From Eqs. (2) to (4) we obtained $M = 2.4 \times 10^9$ and 2.2×10^9 g/mol in 0.05 and 1% poloxamer 188, respectively; the corresponding M-value derived via Eq. (5) from the s-value and the average diffusion coefficient D obtained by DLS were 2.5×10^9 and 2.2×10^9 g/mol, respectively. The agreement between the determined M-values is very good.

4. Discussion

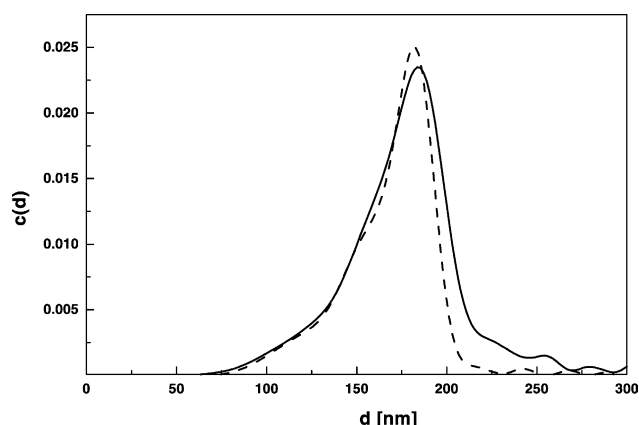As stated in the Introduction, the size and size distribution of nanoparticles to be used as drug delivery

Fig. 6. Particle diameter distribution calculated from the data of Fig. 4b, using a 'solid sphere' model, of samples containing 0.05 % (——) or 1% (– –) poloxamer 188.

systems are important parameters. In this paper we have compared two techniques frequently used for determining particle size, electron microscopy (EM) and DLS, and a third one which is well-known but used less frequently, ANUC, to characterize PBCA nanoparticles.

Of the three techniques, EM, used here in the form of SEM, yields the most direct information on size, size distribution, and shape of the particles. This method gives detailed shape and morphological information that is unique among the three techniques and is highly useful for the evaluation of the data obtained by the other two techniques. One serious disadvantage is the risk of changes in particle properties during drying and contrasting of the sample. In the present study, which used freeze-drying and subsequent Au-shadowing as the preparation method, shrinking of the particles during drying seems to be the most serious risk. The particle diameters determined thus have to be considered as the lower limits of particle size. When employed for the determination of the size distributions of heterogeneous samples, the low number of particles that can be sized and the resulting poor statistics of the method represents another serious disadvantage.

The main advantages of DLS are the short time required to perform the measurements and the relatively low cost of the apparatus. DLS, therefore, has become the preferred method for nanoparticle sizing. It can be very powerful if used carefully. However, the method has several pitfalls, in particular with respect to the influence of dust particles or small amounts of large aggregates in addition to a main component of distinctly smaller size ([20], see also the findings and discussion in [23]). The outcome of the measurements is a distribution of diffusion coefficients D, which then normally is transformed into a distribution of hydrodynamic diameters d_h, i.e. diameters of those spheres which yield the same D-values. This information is of particular value in the case of spherical particles, where d_h will be identical or somewhat larger than the 'real' particle diameter. This is exactly the situation in the present study.

In many chemical companies, sedimentation velocity analysis in the analytical ultracentrifuge has since long been a standard technique for studying size and size distributions of colloidal particles, frequently using non-commercial apparatus [24]. Due to the availability of new software, in particular the $l - s$ $g^*(s)$ method [14,25], analogous analyses can now easily be performed using commercial equipment. In addition, precise measurements of particle density (or its reciprocal, $\bar{v}$) can be obtained at low particle concentrations (see above). Since the movement of particles in a centrifuge shows a stronger size dependence than the diffusion coefficient measured by DLS, the resolution obtained by ANUC is significantly higher and less model-dependent than in DLS [14,25]. The primary result are $g^*(s)$ curves. They then can be converted into concentration-versus-diameter curves for 'equivalent' solid spheres which show the same s-value as the particles studied. As in the case of DLS, these data are of special

interest for spherical particles, where the d-values calculated represent the minimum value the real particle could possess. (In contrast to DLS, the conversion requires knowledge of $\bar{v}$. On the other hand, this knowledge is obligatory anyhow for calculations of molar particle mass.) The necessary information on particle shape again can be obtained by electron microscopy, so that combining the two techniques (as done, e.g. in [13,19,23]) seems to be highly advantageous. In addition, for isolated fractions with narrow size distributions combining the s-value from analytical ultracentrifugation with the D-value from DLS will yield precise molar particle masses via Eq. (5), independent of particle shape.

With respect to the properties of the PBCA nanoparticles, our study obviously has profited from all three techniques. SEM has shown that the particles are virtually perfect spheres, with a minimum mean diameter of approximately 167 nm and a narrow size distribution. DLS has shown that the mean hydrodynamic particle diameter, as judged from two slightly different samples, is between 184 and 199 nm and that different particle preparations are rather similar in size. ANUC has confirmed the narrowness of the size distribution. It has, however, shown that the size distribution is not symmetrical and that a small percentage of the particles has diameters outside the range indicated by SEM. The mean particle diameter according to the 'solid sphere' model was found to be 184 nm. Considering the meaning of the respective diameter values, the agreement between the methods is very good. This in turn suggests that the particles in fact are well-described by the solid sphere model. The ANUC measurements have further yielded the partial specific volume of the particles as 0.871 ml/g and the molar particle mass as around 2.3×10^9 g/mol. The data also demonstrate that the PBCA nanoparticles fulfil the requirements for a useful drug delivery system, with respect to size and size distribution (see Introduction).

Acknowledgements

References

[1] E. Allemann, R. Gurny, E. Doelker, Drug-loaded nanoparticles—preparation methods and drug targeting issues, Eur. J. Pharm. Biopharm. 39 (1993) 173–191.

[2] J. Kreuter, Nanoparticulate systems for brain delivery of drugs, Adv. Drug Deliv. Rev. 47 (2001) 65–81.

[3] A.C. de Verdiere, C. Dubernet, F. Nemati, E. Soma, M. Appel, J. Ferte, S. Bernard, F. Puisieux, P. Couvreur, Reversion of multidrug resistance with polyalkylcyanoacrylate nanoparticles: towards a mechanism of action, Br. J. Cancer 76 (1997) 198–205.

[4] A.E. Gulyaev, S.E. Gelperina, I.N. Skidan, A.S. Antropov, G.Y. Kivman, J. Kreuter, Significant transport of doxorubicin into the brain with polysorbate 80-coated nanoparticles, Pharm. Res. 16 (1999) 1564–1569.

[5] C.E. Soma, C. Dubernet, D. Bentolila, S. Benita, P. Couvreur, Reversion of multidrug resistance by co-encapsulation of doxorubicin and cyclosporin A in polyalkylcyanoacrylate nanoparticles, Biomaterials 21 (2000) 1–7.

[6] A. Friese, E. Seiller, G. Quack, B. Lorenz, J. Kreuter, Increase of the duration of the anticonvulsive activity of a novel NMDA receptor antagonist using poly(butylcyanoacrylate) nanoparticles as a parenteral controlled release system, Eur. J. Pharm. Biopharm. 49 (2000) 103–109.

[7] M.A. El-Egakey, V. Bentele, J. Kreuter, Molecular weights of polycyanoacrylate nanoparticles, Int. J. Pharm. 13 (1983) 349–352.

[8] K. Langer, E. Seegmüller, A. Zimmer, J. Kreuter, Characterization of polybutylcyanoacrylate nanoparticles: I. Quantification of PBCA polymer and dextrans, Int. J. Pharm. 110 (1994) 21–27.

[9] S. Pirker, J. Kruse, C. Noe, K. Langer, A. Zimmer, J. Kreuter, Characterization of polybutylcyanoacrylate nanoparticles. Part II: determination of polymer content by NMR analysis, Int. J. Pharm. 128 (1996) 189–195.

[10] N. Behan, C. Birkinshaw, N. Clarke, Poly n-butylcyanoacrylate nanoparticles: a mechanistic study of polymerisation and particle formation, Biomaterials 22 (2001) 1335–1344.

[11] J. Kreuter, Evaluation of nanoparticles as drug-delivery systems. I: Preparation methods, Pharm. Acta Helv. 58 (1983) 196–209.

[12] P. Sommerfeld, B.A. Sabel, U. Schroeder, Long-term stability of PBCA nanoparticle suspensions, J. Microencapsul. 17 (2000) 69–79.

[13] V. Vogel, K. Langer, S. Balthasar, P. Schuck, W. Mächtle, W. Haase, J.A. van den Broek, C. Tziatzios, D. Schubert, Characterization of serum albumin nanoparticles by sedimentation velocity analysis and electron microscopy, Progr. Colloid Polym. Sci. 119 (2002) 31–36.

[14] P. Schuck, P. Rossmanith, Determination of the sedimentation coefficient distribution by least-squares boundary modeling, Biopolymers 54 (2000) 328–341.

[15] P. Schuck, M.A. Perugini, N.G. Gonzales, G.J. Howlett, D. Schubert, Size-distribution analysis of proteins by analytical ultracentrifugation: strategies and application to model systems, Biophys. J. 82 (2002) 1096–1111.

[16] H.K. Schachman, Ultracentrifugation in Biochemistry, Academic Press, New York, 1959.

[17] C. Tziatzios, H. Durchschlag, B. Sell, J.A. van den Broek, W. Mächtle, W. Haase, J.-M. Lehn, C.H. Weidl, C. Eschbaumer, D. Schubert, U.S. Schubert, Solution properties of supramolecular cobalt coordination arrays, Prog. Colloid Polym. Sci. 113 (1999) 114–120.

[18] C. Tziatzios, A.A. Precup, C.H. Weidl, U.S. Schubert, P. Schuck, H. Durchschlag, W. Mächtle, J.A. van den Broek, D. Schubert, Studies of the partial specific volume of poly(ethylene glycol) derivatives in different solvent systems, Progr. Colloid Polym. Sci. 119 (2002) 24–30.

[19] D. Lochmann, V. Vogel, J. Weyermann, N. Dinauer, H. v. Briesen, J. Kreuter, D. Schubert, A. Zimmer. Physico-chemical characterization of protamine-oligonucleotide nanoparticles Eur. J. Pharm. Biopharm. (2004) (submitted).

[20] B. Berne, R. Pecora, Dynamic Light Scattering—with Applications to Chemistry, Biology, and Physics, Dover Publications, Mineola, NY, 2000.

[21] K. Langer, S. Balthasar, V. Vogel, N. Dinauer, H. von Briesen, D. Schubert, Optimization of the preparation process for human serum albumin (HSA) nanoparticles, Int. J. Pharm. 257 (2003) 169–180.

[22] S.J. Edelstein, H.K. Schachman, The simultaneous determination of partial specific volumes and molecular weights with microgram quantities, J. Biol. Chem. 242 (1967) 306–311.

[23] V. Vogel, J.F. Gohy, B.G.G. Lohmeijer, J.A.van den Broek, W. Haase, U.S. Schubert, D. Schubert, Metallo-supramolecular micelles: studies by analytical ultracentrifugation and electron microscopy, J. Polym. Sci., Part A 41 (2003) 3159–3168.

[24] W. Mächtle, High-resolution, submicron particle size distribution analysis using gravitational-sweep sedimentation, Biophys. J. 76 (1999) 1080–1091.

[25] J. Lebowitz, M.S. Lewis, P. Schuck, Modern analytical ultracentrifugation in protein science: A tutorial review, Protein Sci. 11 (2002) 2067–2079.